Orbital Kondo effect in V-doped $1T$-$CrSe_2$

Matías Núñez,[1,2,3] Daniele C. Freitas,[4,*] Frédérique Gay,[4] Jacques Marcus,[4] Pierre Strobel,[4]
Armando A. Aligia,[1] and Manuel Núñez-Regueiro[4]

[1]*Consejo Nacional de Investigaciones Científicas y Técnicas, Buenos Aires, Argentina*
[2]*Dpto. Materiales Nucleares, Centro Atómico Bariloche, Comisión Nacional de Energía Atómica, 8400 Bariloche, Argentina*
[3]*Instituto de Ciencias Básicas, Universidad Nacional de Cuyo, Mendoza, Argentina*
[4]*Institut Néel, Université Grenoble Alpes and Centre National de la Recherche Scientifique 25 rue des Martyrs, BP 166, 38042, Grenoble cedex 9, France*

(Received 20 September 2013; published 26 December 2013)

We have studied the resistance of $1T$-$CrSe_2$, as the Cr atoms are substituted by V or Ti. The V replacement leads to a logarithmic increase in the resistance as the temperature is lowered, proportional to the V concentration. While this behavior is consistent with the Kondo effect, the weak dependence of the resistance with magnetic field and the fact that the system has antiferromagnetic order, rule out a Kondo effect due to spin degeneracy. In contrast to the case of V, Ti substitution does not increase the logarithmic term while application of pressure destroys it. Calculations of the electronic structure within the framework of density functional theory, maximally localized Wannier functions, and many-body calculations in a cluster containing a Cr or V atom and its six nearest-neighbor Se atoms, helped to reveal the existence of an orbital Kondo effect due to orbital degeneracy in the V substitutional impurities.

DOI: 10.1103/PhysRevB.88.245129 PACS number(s): 75.50.Ee, 71.20.Be

I. INTRODUCTION

Layered compounds of $3d$ transition metals have been studied intensively during recent years because of their interesting properties, such as superconductivity with high critical temperatures in the cuprates[1,2] and iron pnictides.[3] Layered hexagonal cobaltates Na_xCoO_2 have attracted interest due to the high thermopower and at the same time low thermal conductivity and resistivity for $0.5 < x < 0.9$,[4,5] and the discovery of superconductivity in hydrated Na_xCoO_2.[6] Recently a theory for this superconductivity was proposed,[7] using an effective model for the t_{2g} orbitals of Co.[8] An effective model which includes all $3d$ orbitals has been recently studied.[9]

As Na_xCoO_2, $1T$-$CrSe_2$ also has a hexagonal structure of transition-metal cations, surrounded by anions in an array of edge-sharing $CrSe_6$ (instead of CoO_6) octahedra. An important difference, however, is that $1T$-$CrSe_2$ is antiferromagnetically ordered at room temperature.[10] In fact the search for a material with high Néel temperature and low spin is also expected to have a large superconducting critical temperature from a magnetic superconducting mechanism, and this motivated a previous study of magnetic properties in this system, as well as the effect of different dopants on the magnetic order.[10]

The Kondo effect is one of the most paradigmatic phenomena in strongly correlated condensed matter systems.[11] The Kondo model, originally proposed by Kondo to explain the resistance minimum and a logarithmic dependence on temperature $\log(T)$ of the resistivity at low temperature T in dilute magnetic alloys,[12] is still a subject of great interest. In its simplest version, the phenomenon is characterized by the emergence of a many-body singlet ground state formed by an impurity spin $1/2$ and the spin $1/2$ of the conduction electrons near the Fermi level, below the characteristic Kondo temperature T_K. The effect is destroyed by application of a magnetic field B such that $\mu_B B > k_B T_K$, which breaks the degeneracy between spin up and down at the impurity.

The role of the impurity spin can be replaced by other quantum degrees of freedom (pseudospin) that distinguish degenerate states, such as two-level systems,[13] or orbital momentum. Orbital degeneracy leads to the orbital Kondo effect or to more exotic Kondo effects, such as the SU(4) one, when both orbital and spin degeneracy coexist. Some examples are present in nanoscopic systems.[14–25] Evidence of the orbital Kondo effect has also been inferred from the observation of a resonance near the Fermi energy in scanning tunneling microscopy studies of the Cr(001) surface and its theoretical interpretation.[26,27] In this system, the Kondo resonance comes as a result of the degeneracy between surface $3d$ states of xz and yz symmetry, where z is the direction perpendicular to the surface. Spin degeneracy is not possible, since the Cr(001) surface is ferromagnetic. More recently, orbital Kondo resonance peak has been observed in photoemission studies of V-doped Cr.[28]

In this work, we report on measurements of resistance in V- and Ti-doped $1T$-$CrSe_2$, and calculations on the electronic structure of the system. V doping leads to a $\log(T)$ dependence of the resistance, proportional to the V concentration, which is consistent with the Kondo effect.[12] However, this Kondo effect cannot be due to spin degeneracy, since the system is magnetically ordered.[10] Our calculation of maximally localized Wannier functions (MLWFs), from density-functional theory (DFT) calculations as well as the exact solution of local VSe_6 and $CrSe_6$ clusters with all correlations inside the d shell included, indicate that the observed behavior in the resistance is due to an orbital Kondo effect. This conclusion is also supported by the weak dependence of the $\log(T)$ term with the applied magnetic field. Pressure destroys this term, probably by breaking the orbital degeneracy.

The paper is organized as follows. In Sec. II we report on the experimental results for the resistivity and a preliminary

analysis on them. Section III contains the DFT, MLWF, and cluster calculations which help to elucidate the electronic structure of the system. Section IV is a summary and discussion. Some details about the symmetry of the orbitals in appropriate basis are left to an Appendix.

II. EXPERIMENT

The $1T$-$Cr_{1-x}V_xSe_2$ and $1T$-$Cr_{1-x}Ti_xSe_2$ compounds ($0 \leqslant x \leqslant 0.5$) were synthesized indirectly by oxidation of $ACr_{1-x}V_xSe_2$ and $ACr_{1-x}Ti_xSe_2$, A = K or Na. This method was used before by Van Bruggen *et al.*[29] to obtain $CrSe_2$ from K_xCrSe_2, $x \simeq 1$. The parent compounds were prepared by a molar mixture of the elements under argon atmosphere in a glovebox. This mixture was then heated to the melting point of both the alkaline and selenium, then kept at 700 °C for five days in an evacuated quartz tube. The tubes were opened in a glovebox in order to prevent oxidation. The formation of the $A(Cr,M)Se_2$ (M = V or Ti) parent compound was confirmed by x-ray powder diffraction. Alkaline atom deintercalation was then carried out by reacting the sodium parent compounds in solutions of iodine in acetonitrile. These suspensions were stirred for approximately 1 h, using an excess of iodine. The final product was washed with acetonitrile to remove the iodide formed, filtered, and then dried under vacuum. A mixture of brilliant dark-gray platelets about 100 μm diameter and black powders with a metallic cluster were obtained.

The magnetic properties of our samples were described in Ref. 10. In the undoped compound $CrSe_2$, the magnetic Cr ions order antiferromagnetically in the hexagonal planes perpendicular to the c direction (the z axis) and ferromagnetically in the c direction. On Ti substitution, the magnetic order evolves into ferromagnetism, while V substitution maintains antiferromagnetism, albeit at a lower transition temperature. The different effects of the substitutional ions have been interpreted in terms of the corresponding change in the ratio of lattice parameters c/a and its consequences on the effective exchange parameters.[10]

In order to perform electrical resistance measurements we compacted the powder into bars of similar shape, by cold pressing at room temperature. Due to the inhomogeneous granularity of the powder, bars of the same preparation had resistivities could change within 30%. In order to circumvent these differences that arise from an unknown geometrical coefficient due to the different filling factors, normalization to the room temperature value was used. We show in Fig. 1 the electrical resistance, normalized to the room temperature value, for all the samples with different doping content, in order to clearly show the relative variation. Already for the pure $CrSe_2$, we observe, instead of the linear in temperature dependence expected for a metallic sample, a rather constant behavior down to about 100 K. Below this value the resistance slightly increases as the temperature T decreases. This behavior may partly be due to scattering against impurities produced by the stacking disorder present in our samples, a consequence of the indirect method of preparation. The behavior is similar to that reported previously for pure $CrSe_2$ (Ref. 29). Titanium substitution has a small effect on the resistance of the samples, with a small reduction of its value at low temperatures.

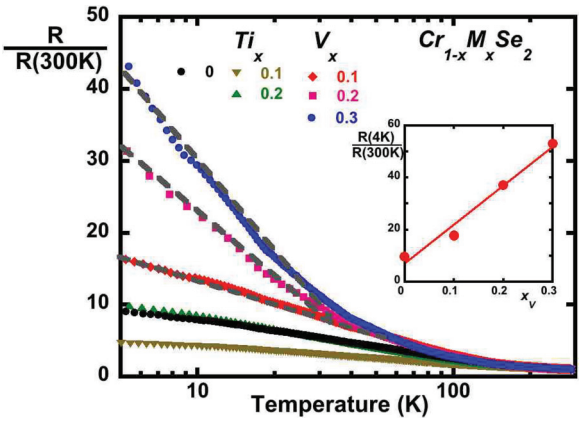

FIG. 1. (Color online) Electrical resistance, normalized to its value at room temperature, as a function of temperature. Straight lines are drawn to show the $\log(T)$ dependence. The inset shows the dependence on the C content x_V.

In contrast, vanadium substitution induces a dramatic increase in the low temperature resistance. The magnitude of the effect, measured by the value of the 4 K resistance, is directly proportional to the vanadium concentration, as shown in the inset of Fig. 1. The curves are plotted in a logarithmic scale for the temperature T, as we have found that a $\log(T)$ is what best fits the low temperature data. No activated behavior, e.g., two-dimensional (2D) or three-dimensional variable range hopping dependence, can fit the data for over one decade as does $\log(T)$. This temperature dependence is expected for Kondo type carrier scattering against isolated magnetic impurities, even though the magnetization measurements do not furnish evidence for isolated moments.[10]

As anticipated in the Introduction, this behavior is consistent with an orbital Kondo effect. Formally the oxidation state of Cr in $CrSe_2$ is Cr^{4+}, which has two electrons in the $3d$ shell. The magnetism of the system is consistent with a physical picture in which these two electrons occupy two orbitally degenerate states with the same spin, forming a spin triplet and an orbital singlet.[10] When Cr^{4+} is replaced with V^{4+}, with only one $3d$ electron, this electron can occupy any one of the degenerate states building an orbital doublet, which can give rise to the orbital Kondo effect. Instead, Ti^{4+} has no $3d$ electrons and does not act as an orbital impurity. The residual $\log(T)$ for pure $CrSe_2$ might be due to a small amount of Cr^{5+} or Cr^{3+} impurities. While, as we shall show, the charges given by an ionic model are too large, this picture retains basic physics and the resulting quantum numbers are correct.

We have measured the effect of a magnetic field on the resistance. For an ordinary Kondo effect due to screening of a spin degree of freedom, the effect and the increase in resistivity at low temperatures are strongly suppressed by a magnetic field H. We show in Fig. 2 that the effect of H is extremely small, only a few parts per thousand. Furthermore, resistance increases with magnetic field, instead of decreasing as in a standard Kondo effect. The observed positive magnetoresistance also excludes another possible explanation for the $\log(T)$ dependence, namely, weak 2D localization that should have given a negative magnetoresistance. It has been shown in Ref. 10 that V doping maintains the antiferromagnetic order,

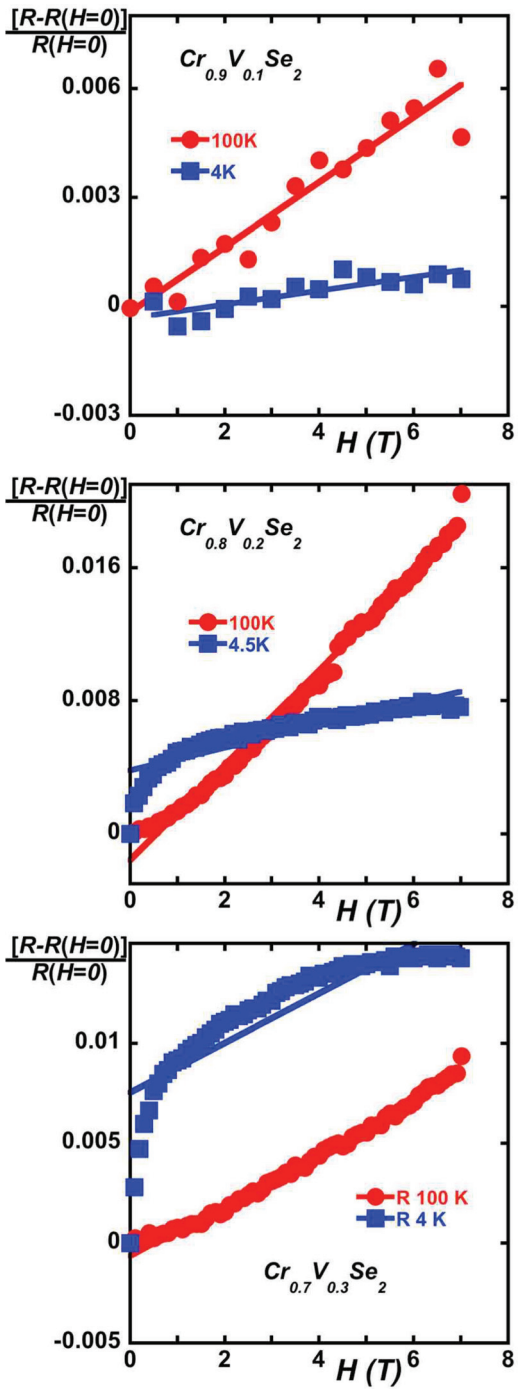

FIG. 2. (Color online) Normalized magnetoresistance as a function of magnetic field.

and as a result the spin of the V^{4+} should be pinned down by the antiferromagnetic order. Instead, as we shall show in Sec. III, the V impurities have an orbital degree of freedom between two possible degenerate states. Thus, an orbital Kondo effect seems to be the most plausible explanation for our data.

We have fitted our data for the V-doped samples with the known expression for the Kondo resistance:[30]

$$\rho_K(T) = \frac{\rho_U}{2}\left\{1 - \frac{\ln\left[(T^2+\theta^2)/T_K^2\right]^{1/2}}{\pi[S(S+1)]^{1/2}}\right\}, \qquad (1)$$

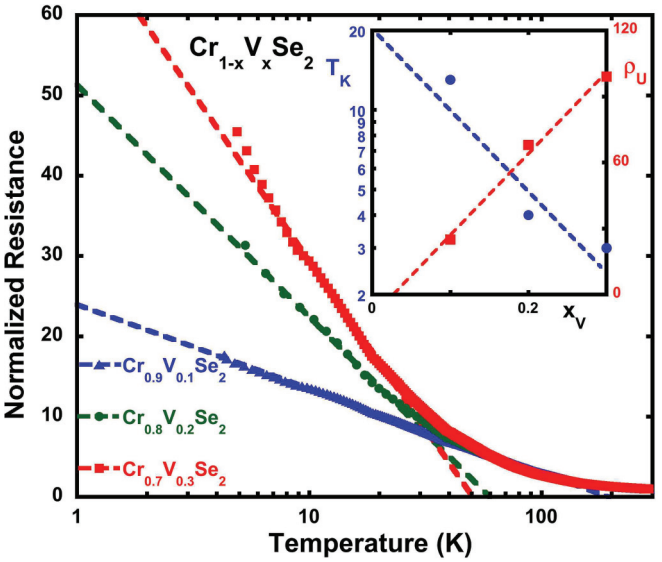

FIG. 3. (Color online) Fit using Eq. (1) to the normalized electrical resistance of V-doped samples. Inset: the variation of both the Kondo temperature T_K and the unitary limit resistance ρ_U with vanadium content.

where T_K is the Kondo temperature, ρ_U represents the unitarity-limit resistivity, and $\ln(\theta/T_K) = -\pi[S(S+1)]^{1/2}$, namely, $\theta = 0.066T_K$ for $S = 1/2$.[30] From this fit we obtain that the Kondo temperature decreases with increasing vanadium content (inset of Fig. 3). We remind the reader that the Kondo temperature $T_K \sim \exp[-1/N(E_F)J]$, where $N(E_F)$ is the density of states at the Fermi level and J the exchange interaction. Thus the dependence of T_K with V content is probably due to small changes in either $N(E_F)$ or J due to changes in c/a which affect the antiferromagnetism and the electronic structure.[10] As expected for an impurity effect, the coefficient of the Kondo term increases linearly with the V concentration. Thus, our data can be explained by a Kondo effect, albeit of possible orbital origin, as the magnetoresistance precludes a standard Kondo effect.

We have also studied the effect of pressure on the resistance of some of our samples up to 15 GPa using Bridgman anvils as described in Ref. 31. We observe (Fig. 4) a monotonous decrease of the resistance towards a usual metallic dependence at higher pressures, i.e., the $\log(T)$ disappears with pressure. This evolution is also consistent with a Kondo effect of orbital origin, as pressure probably produces distortions of the lattice that split the orbital degeneracy necessary for an orbital Kondo effect.

Summarizing, from our results we observe that replacement of Cr by V induces a strong logarithmic term proportional to the vanadium concentration, while replacement by Ti does not have an important effect on the resistance. This suggests that V (but not Ti) has some intrinsic degeneracy that leads to the Kondo effect. It cannot be spin because a normal Kondo effect is precluded by the measured magnetoresistance. The simplest hypothesis that can explain our results is thus an orbital Kondo effect. This is explored in the next section.

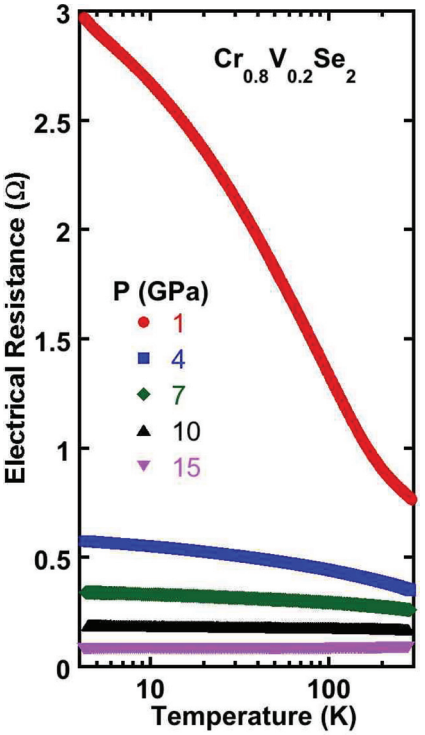

FIG. 4. (Color online) Electrical resistance of a $Cr_{0.8}V_{0.2}Se_2$ sample as a function of temperature for various pressures.

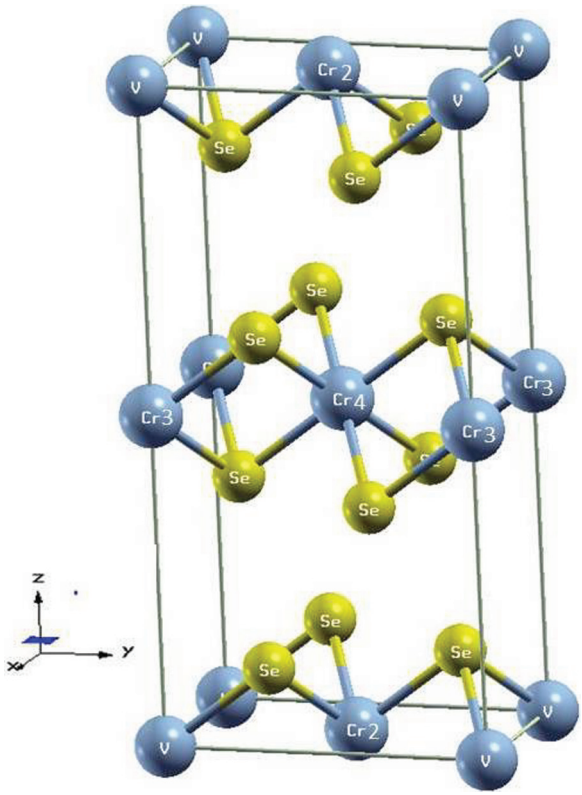

FIG. 5. (Color online) Unit cell of Cr_3VSe_8 used in the DFT calculations.

III. THEORY

As a starting point for the theoretical analysis, we have calculated the electronic structure of the system within the framework of DFT.[32] The information from this calculation, in particular the total charge in the MLWF of $3d$ character, and the Cr-Se and V-Se hopping, was used in the exact diagonalizations of $CrSe_6$ and VSe_6 clusters in which all correlations inside the $3d$ shell were included. In all calculations, the experimental lattice parameters of $CrSe_2$ were used.[10] None of these calculations alone can describe the Kondo effect. Correlations are absent in the DFT calculations, and the extended states near the Fermi surface cannot be described in a cluster calculation. However, our results show that the ground state of the VSe_6 cluster is an orbital doublet of localized nature, which should lead to a Kondo effect when the hybridization with the extended states is included. The $CrSe_6$ clusters are in an orbital singlet configuration and therefore do not polarize the VSe_6 doublet.

These arguments depend on the symmetry of the orbitals involved and their ordering. The local symmetry around a Cr atom in $CrSe_2$ (or an isolated substitutional V impurity) is given by the point group D_{3d}. We define the z axis along the C_3 axis, in the c direction of the crystalline structure and choose the x axis in the direction of two nearest-neighbor Cr atoms in the xy plane. Note that then, taking the origin of coordinates at a Cr atom, one of its nearest-neighbor Se atoms lies in the yz plane (see Fig. 5). With this choice of axis, the $3d$ orbital $3z^2 - r^2$ transforms like the a_{1g} representation of D_{3d}, while the pairs (xz, yz) and $(xy, x^2 - y^2)$ transform like the double degenerate e_g representation. In an oversimplified picture, we could state that before the Kondo screening (at high temperatures) takes place, a V^{4+} ion introduced as a substitutional impurity, has one electron with fixed spin given by the antiferromagnetic interaction with its Cr^{4+} neighbors, that occupies one of two degenerate orbitals: either $\alpha xz + \beta xy$ or $\alpha yz + \beta x^2 - y^2$. The Kondo effect then leads to an orbital singlet. This effect is not possible if the electron would occupy the nondegenerate $3z^2 - r^2$ orbital. The calculations of this section were motivated by the need to confirm or rule out the above picture.

A. DFT calculations

We used the quantum ESPRESSO code[33] that uses a plane-wave basis to describe the electronic wave functions and ultrasoft pseudopotentials to represent the interaction between electrons and ions.[34] The exchange and correlation potential was considered at the level of the generalized gradient approximation based on the Perdew-Burke-Ernzerhof expression.[35] Previously,[10] we have found that the results using the local density approximation[36,37] were very similar.

We have made two different calculations. In the first one, for pure $CrSe_2$, a simple orthorhombic supercell containing two elementary cells (six atoms) was used. This calculation reproduces the experimentally observed[10,38] collinear order of less energy, which is antiferromagnetic in the xy planes and ferromagnetic between planes. Details of these calculations can be found in Ref. 10.

We have to note that spins 1 in a triangular lattice may have noncollinear antiferromagnetic order or even form a spin liquid.[39] However the type of magnetic order is not essential

for our discussion, as long as the V spins are not free to rotate under an applied magnetic field.

The second calculation had the purpose of studying the electronic structure near V impurities. Thus an orthorhombic supercell for the hypothetical compound Cr_3VSe_8 was built (see Fig. 5), in which the original unit cell of $CrSe_2$ is doubled in the xy plane (as in the calculation explained above) as well as in the z direction. This is the same kind of supercell used in Ref. 10. Details about the convergence parameters can be found there, although a denser mesh was used in this case for the reciprocal space integrations. In particular, a $(12 \times 12 \times 12)$ Monkhorst-Pack mesh[40] was needed for convergence of the localization of the MLWFs. The V content in Cr_3VSe_8 is not in the dilute limit, but larger unit cells are numerically too expensive for our analysis based on the MLWFs. In addition, signatures of the Kondo effect in the resistivity persist for a V concentration of 0.3.

The MLWFs were obtained with the algorithms originally proposed by Marzari and Vanderbilt[41] as implemented in the WANT code.[42] A disentanglement procedure[43] was applied before starting the localization algorithm. From the well converged MLWFs, a projection of the density of states on the Wannier functions was performed. The electronic charge associated with each MLWF was obtained by integration of the corresponding local-Wannier-function density of states (PWfDOS) up to the Fermi level. The total charge on the Wannier functions of $3d$ symmetry and the Cr-Se and V-Se matrix elements were used in the cluster calculations of Sec. III B.

In Fig. 6 we show the calculated band structure for Cr_3VSe_8. The energy range shown contains all the bands with $3d$ and $4p$ nature. We used that energy window in order to obtain all the $3d$ type MLWFs belonging to Cr and V and $4p$ type MLWFs belonging to Se atoms. We tried to obtain a set of MLWFs for the $3d$ bands alone using a restricted energy window and the disentanglement procedure,[43] but the procedure failed due to the large covalency between transition metals and Se atoms. By using a larger energy window and despite the increased number of wave functions included in this way (20 $3d$ functions and 24 $4p$ functions for each spin) the minimization of the spatial spread of the Wannier functions was achieved and a well behaved set of MLWFs was obtained. Drawing maps of constant value for the different $3d$ MLWF, we found that they correspond to symmetry $3z^2 - r^2$, $x^2 - r^2$, xy, yz, and xz . The matrix elements between different MLWFs also respect the expected symmetry.

The projection of the density of states on this set of MLWFs (PWfDOS) can be seen in Fig. 6. The contribution of all d states and p type orbitals is shown separately. The sum of both in that energy range equals the total DOS. The peak near 2 eV corresponds to $3d$ states of symmetry e_g^O for a (hypothetical) O_h symmetry (see the Appendix for a discussion on symmetry), while the t_{2g} states lie slightly below the Fermi energy (which we choose as the zero of energy).

In Fig. 7 we show the total spectral density of $3d$ character corresponding to the MLWFs of the four transition-metal atoms of the unit cell. Note that due to the antiferromagnetic order, the majority spin in V and Cr3 (Cr2 and Cr4), which lie one above the other in the z direction is up (down). While the introduction of the V atoms in the supercell breaks the

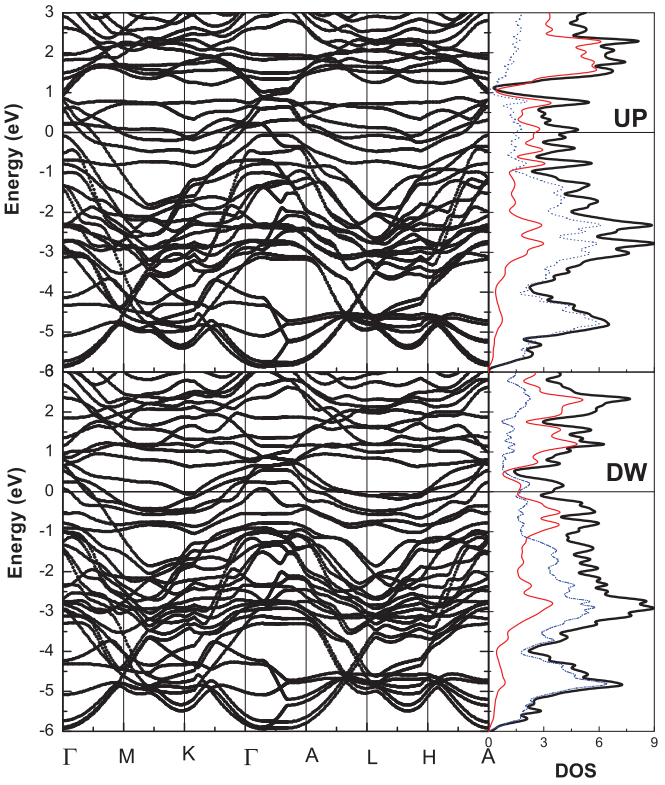

FIG. 6. (Color online) Electronic band structure calculated with DFT (left) and corresponding total density of states (thick black line on the right) for spin up (top) and spin down (bottom). Projection of the DOS on the MLWFs with $4p$ character (blue dot-dashed line) and on $3d$ type MLWFs (red thin line) are also shown.

threefold symmetry C_3 around the z axis the former degenerate e_g states xz, yz, and xy, $x^2 - y^2$ continue to lie approximately at the same energy. The peaks which are above the Fermi energy for V correspond to states of t_{2g} symmetry (see the Appendix), mainly xy, $x^2 - y^2$, and $3z^2 - r^2$. These peaks are shifted to about -0.6 eV (1.7 eV) for the majority (minority) spin of the Cr atoms. As can be inferred from an inspection of the weight of the spectral density below the Fermi energy, the spin polarization of the V atoms is less than that of the Cr atoms. We will return to this point later. The peaks near -2.7 eV are of e_g^O symmetry and correspond to a small admixture of $3d$ character in the $4p$ Se bands of the same symmetry.

The details of the peaks in the spectral densities near the Fermi energy, separated by symmetry, are shown in Fig. 8. Clearly these peaks correspond mainly to states of t_{2g} symmetry. This is expected if one considers the character of the states at low energy of a perfect VSe_6 or $CrSe_6$ octahedron, and treats the distortion as a perturbation. This is explained in the Appendix. As explained there, the t_{2g} states are the $d_{3z^2-r^2}$, and the degenerate e_g states in D_{3d} symmetry: a linear combination of mainly xy and some part of d_{xz} and its partner, $x^2 - y^2$ plus some d_{yz}. The total weight below both peaks is slightly above two electrons. For V the most intense peak corresponds to the $x^2 - y^2$ Wannier function which is about two times larger than the xy contribution. The fact that the former is more intense is due to a loss of D_{3d} symmetry due to the effect of nearest V atoms (see Fig. 5), which is not expected for dilute V concentrations. We also expect that random distribution of

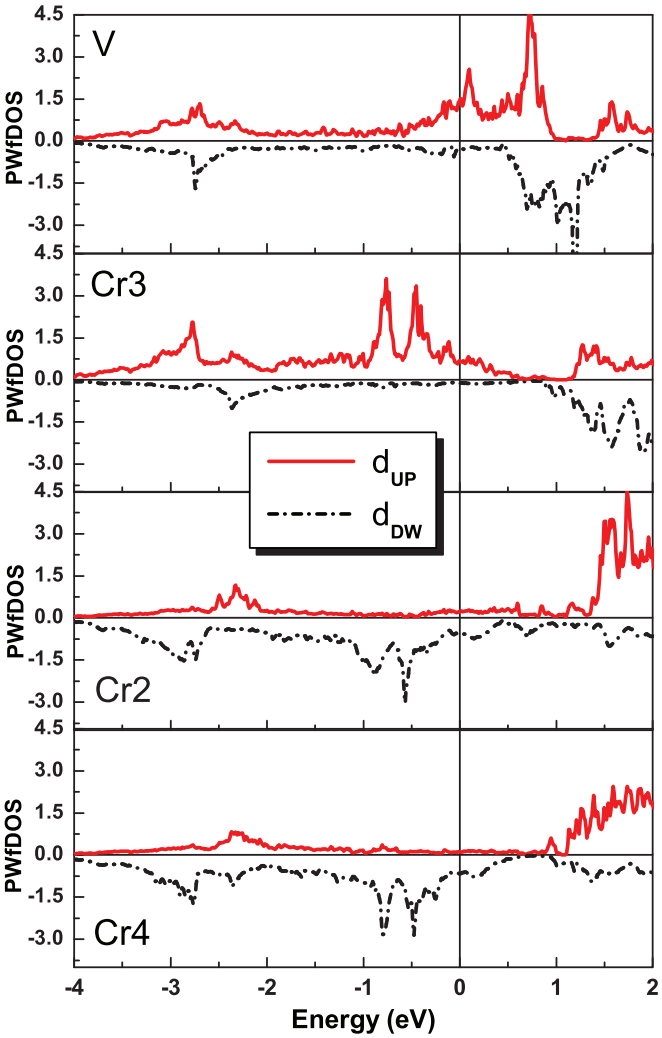

FIG. 7. (Color online) Projection of the DOS on the spin up and spin down MLWFs associated with $3d$ states belonging to the nonequivalent atoms in the unit cell (see Fig. 5).

V substitutes has a less pronounced effect in breaking the symmetry. The intensity of the $d_{3z^2-r^2}$ peak lies between these two. This already points out that V prefers to occupy states of e_g character.

For Cr3, which has the same majority spin as V, the structure of the peaks is similar, but in contrast to V, the weight of the $d_{3z^2-r^2}$ Wannier function is slightly larger than that of the $x^2 - y^2$ one. The most important difference is that the peaks for spin up (down) lie almost completely below (above) the Fermi energy. Naturally, the occupations of the spins are inverted for the other two Cr atoms in the unit cell, which have the majority spin down (see Fig. 7).

The V peaks near 0.1 and 0.7 eV suggest the presence of a localized state of V. The hopping between nearest-neighbor V atoms, absent for dilute systems, has a broadening effect on the peak. Therefore, it should be sharper for small V concentrations. However, an aspect which is in principle unexpected, is the small spin polarization of the V atoms. In Table I we display the values of the occupations of the different MLWFs (orbitals) and compare it with the corresponding one for the many-body cluster calculation explained in Sec. III B.

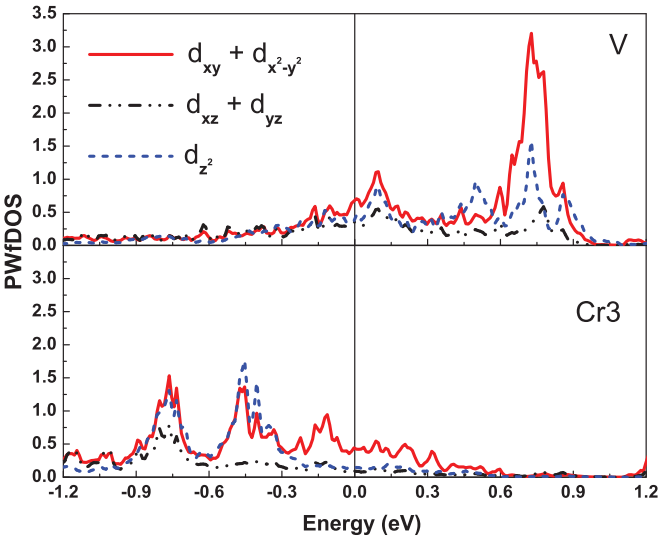

FIG. 8. (Color online) Projection of the DOS on the spin up $3d$ type MLWFs associated with V and Cr. The PWfDOS of d_{xz} and d_{yz} (d_{xy} and $d_{x^2-y^2}$) are added and shown by a red full (black dashed) line, while the PWfDOS for $d_{3z^2-r^2}$ is shown by a green dot-dashed line.

The total spin polarization is 0.54 electrons in DFT and 1.17 in the ground state of the cluster. For comparison, we show in Table II the occupations that correspond to a Cr atom in $CrSe_2$. In this case, there is very good agreement with the cluster calculation.

A possible reason for the low spin polarization for the V atom while using the local spin density approximation is the soft Hund's-like exchange interaction of the exchange and correlation functional. In order to check this, we have made a calculation with LSDA + U,[44] as implemented in QUANTUM ESPRESSO[45] in a larger unit cell. We used $U = 3.5$ eV for V and $U = 4$ eV for Cr. The resulting total spin polarization that results from the Löwdin charges is 1.59 electrons, which compares well with 1.17 electrons as the spin polarization for the d shell according to the cluster calculation (Table I). For comparison, the same calculation for the Cr atoms gives a total spin polarization of 3.20 electrons (two times that of V), while the MLWF in LSDA gives for the $3d$ shell 2.51 and the cluster calculation 2.29 (Table II), near two times the corresponding result for V. The reader might ask if it were not more convenient to use also LSDA + U as an input for the calculation with MLWF. We preferred to use LSDA because of the limitations of LSDA + U for metallic systems, some of which are discussed by Mazin *et al.*[46] In any case, the parameters used for the cluster calculation (total $3d$ charge and hopping parameters) are rather insensitive to the change of functional.

TABLE I. Occupation of the different $3d$ orbitals of V in Cr_3VSe_8.

Orbital	$3z^2 - r^2$	xz	yz	xy	$x^2 - y^2$
MLWF spin up	0.402	0.409	0.418	0.411	0.372
Cluster spin up	0.326	0.553	0.363	0.783	0.301
MLWF spin down	0.266	0.342	0.349	0.242	0.274
Cluster spin down	0.213	0.256	0.281	0.188	0.222

TABLE II. Occupation of the different $3d$ orbitals of Cr in $CrSe_2$.

Orbital	$3z^2 - r^2$	xz and yz	xy and $x^2 - y^2$
MLWF spin up	0.902	0.584	0.744
Cluster spin up	0.843	0.576	0.722
MLWF spin down	0.147	0.263	0.173
Cluster spin down	0.173	0.273	0.213

B. Cluster calculations

In this section, we calculate the ground state and the first excited state of a cluster containing either a V or a Cr atom and its six nearest-neighbor Se atoms, with open boundary conditions. All correlations inside the $3d$ shell of V or Cr are included in the exact diagonalization, as described in Refs. 47 and 48. The main idea behind this calculation is that effective Hamiltonians that describe exactly the local physics can be constructed from Wannier functions of Se atoms centered at the transition-metal ones, as done in the cuprates.[49–53] While we are not using these wave functions, the main physics is contained in the cluster and the error comes from the overlap of the wave function of different clusters with common Se atoms,[47] which can be estimated in an approach using nonorthogonal orbitals,[54] and decreases with increasing number of ligand neighbors to the transition-metal ion. In any case, our goal here is to see what is the effect of the neighboring Se on the degeneracy of the $3d$ levels, and this cluster is appropriate for this.

The main question is what happens with the t_{2g} orbitals of the regular octahedron (with point group symmetry O_h) as the symmetry is reduced to that of the real structure D_{3d}. As discussed in the Appendix, the three t_{2g} states split into an a_{1g} singlet and an e_g doublet. In a ionic picture, V^{4+} has one electron that occupies the lowest level. If the latter were the nondegenerate a_{1g} state, since the spin degeneracy is broken by the magnetic field, the Kondo effect would not be possible.

For the orbital Kondo effect to take place, it is also necessary that the neighboring Cr^{4+} ions are orbital singlets. Otherwise the orbital degeneracy at the V site would be broken by effective V-Cr orbital exchange terms analogous to the spin-exchange ones.[55] In other words, if in Cr^{4+} one electron occupies the nondegenerate a_{1g} orbital, and the other one is in one of the degenerate e_g orbitals, the ion is a spin triplet and an orbital doublet, and one expects spin and orbital ordering, as theoretically discussed for example in RuO_2 planes in $RuSr_2(Eu,Gd)Cu_2O_8$.[56] Therefore, one needs to know the symmetry of the ground state for both $CrSe_6$ and VSe_6 octahedra for the realistic geometry, or in simpler terms, the sign of the t_{2g} splitting.

The most reliable methods to calculate this splitting are the configurational-interaction quantum-chemistry ones,[57] while estimations based on fitting of DFT bands usually underestimate the splitting, probably due to the shortcomings of DFT to account for orbital polarization.[58–60] Our cluster calculation neglects interatomic repulsions and with them the contribution of Madelung potentials to the crystal-field splitting, but they are expected to play a minor role in covalent materials, for which this splitting is dominated by the hopping of electrons between these ions and their nearest ligands.[61] In the case Na_xCoO_2, for which the structure of the CoO_6 clusters (compressed along z instead of expanded) is similar to that of the $CrSe_6$ clusters in $CrSe_2$, the results for the splitting using our approach[48] are in qualitative agreement with quantum-chemistry ones,[57] but differ from those obtained from DFT, which have opposite sign. Only the former results are consistent with the observed Fermi surface in Na_xCoO_2.[8,48]

The model for the cluster describes the $3d$ electrons of the transition metal (Cr or V) and the $4p$ electrons of the Se atoms, located at the positions determined by the structure of $CrSe_2$.[10] The relevant filling for the calculation in the $CrSe_6$ cluster corresponds to formal valences Cr^{4+} (two $3d$ electrons) and Se^{2-} (six $4p$ electrons per Se atom), a total of 38 electrons. This is equivalent to eight holes added to the vacuum state which corresponds to full $3d$ and $4p$ shells in all atoms. For the VSe_6 cluster one more hole should be added.

The Hamiltonian for the clusters takes the form

$$H = \sum_{\alpha\in e_g^O,\sigma} \epsilon_{e_g^O} d^\dagger_{\alpha\sigma} d_{\alpha\sigma} + \sum_{\beta\in t_{2g},\sigma} \epsilon_{t_{2g}} d^\dagger_{\beta\sigma} d_{\beta\sigma} + H_I + \sum_{j\eta\sigma} \epsilon_{\mathrm{Se}} p^\dagger_{j\eta\sigma} p_{j\eta\sigma} + \sum_{j\eta\xi\sigma} t_j^{\eta\xi} (p^\dagger_{j\eta\sigma} d_{\xi\sigma} + \mathrm{H.c.}). \quad (2)$$

The operator $d^\dagger_{\xi\sigma}$ creates a hole on the $3d$ orbital ξ with spin σ. Similarly $p^\dagger_{j\eta\sigma}$ creates a hole on the $4p$ orbital η at Se j with spin σ. The first two terms correspond to the energy of the e_g^O and t_{2g} orbitals of a regular $CrSe_6$ octahedron (see the Appendix for the details on symmetry and the effect of the expansion along the z direction). The most important physical ingredients are the interactions inside the $3d$ shell H_I and the hopping $t_j^{\eta\xi}$, parametrized as usual, in terms of the Slater-Koster parameters $(pd\sigma)$ and $(pd\pi)$.[62] We include the part of the cubic crystal field splitting $\epsilon_{t_{2g}} - \epsilon_{e_g^O} = 10Dq$, which is due to interatomic interactions, as a parameter. The part of this splitting which is due to covalency is larger (about 2 eV) and is included in the calculation.

H_I contains all interactions between d holes assuming spherical symmetry [the symmetry is reduced to O_h by the cubic crystal field $10Dq$ and to D_{3d} by the last (hopping) term of Eq. (2)]. The expression of H_I is lengthy and we do not reproduce it here. It is included in the Appendix of Ref. 48 and more details on its derivation are given in Ref. 47. All interactions are given in terms of three free parameters $F_0 \gg F_2 \gg F_4$. For example, the Coulomb repulsion between two holes or electrons at the same $3d$ orbital is $U = F_0 + 4F_2 + 36F_4$, and the Hund rules exchange interaction between two e_g^O (t_{2g}) electrons is $J_e = 4F_2 + 15F_4$ ($J_t = 3F_2 + 20F_4$).

The parameters of the model are determined as follows. We take $F_2 = 0.16$ eV, $F_4 = 0.011$ eV, which fit the low-energy spectra of $3d$ transition-metal atoms. We use $F_0 = 3$ eV, leading to $U \approx 4$ eV, a typical value for early $3d$ transition metals. For the $CrSe_6$ cluster, $(pd\pi) = 0.5$ eV was determined from the (approximate) average between spin up and down, of the hopping between the $3d_{xz}$ Wannier function obtained in the DFT calculation, and the $4p_x$ one of the Se atom in the $(0, \cos\theta, \sin\theta)$ direction, where $\theta \approx 37^\circ$ is the angle between this Cr-Se bond and the xy plane. This matrix element is

TABLE III. Occupation of the different $3d$ orbitals of Cr for the low-lying states of the $CrSe_6$ cluster.

Orbital	$3z^2-r^2$	xz	yz	xy	x^2-y^2
a_{1g} spin up	0.592	0.632	0.632	0.793	0.793
Spin down	0.233	0.267	0.267	0.188	0.188
e_g xz spin up	0.969	0.602	0.493	0.830	0.544
Spin down	0.143	0.263	0.290	0.197	0.254
e_g yz spin up	0.969	0.493	0.602	0.544	0.830
Spin down	0.143	0.290	0.263	0.254	0.197

independent of $(pd\sigma)$. From the hopping between the $3d_{yz}$ and $4p_y$ Wannier functions of the same bond, we determine $(pd\sigma) = -1.5$ eV. In the V case, the corresponding values are $(pd\pi) = 0.6$ eV, $(pd\sigma) = -1.65$ eV. The parameter $10Dq = 0.5$ eV was chosen to give approximately the distribution between $3d$ e_g^O and t_{2g} holes determined by the DFT results in $CrSe_2$. We took the same value in the V calculation since the results are rather insensitive to this parameter. Finally ϵ_{Se} was determined fitting the total charge in the $3d$ shell that results from the DFT calculations. The resulting values were $\epsilon_{Se} = 14.0$ eV for $CrSe_6$ and 17.6 eV for VSe_6.

The resulting ground state for the $CrSe_6$ cluster has spin 1 and a_{1g} symmetry (invariant under the operations of D_{3d}). It has the same symmetry of the state of Cr^{4+} ion, in which two electrons occupy with the same spin, the two partners of an e_g doublet (one with xz and the other with yz symmetry). Although this ionic limit does not represent the distribution of charges of the actual ground state, displayed in Table III, both states are connected adiabatically by a change in the energy of the Se orbitals, ϵ_{Se}, which controls the degree of covalency. Therefore, the ionic picture is qualitatively correct. A similar situation takes place in the cuprates,[49–53] and in Na_xCoO_2,[8,47] where in spite of the large covalency with O atoms, effective models which contain only "dressed" transition-metal states describe adequately the physics. In the cuprates, optical properties related with O atoms were calculated using these one-band models.[53,63] The large degree of covalency is evident from the distribution of the eight holes among Cr and Se orbitals. For the regular octahedron (symmetry O_h; see the Appendix for details on symmetry), 2.96 holes are in $3d$ t_{2g} orbitals, and 1.04 in Se orbitals of the same symmetry. For the e_g^O orbitals, 2.46 holes are in Cr and 1.54 in Se $4p$ orbitals. In other words, compared with the extreme ionic limit with 4 $3d$ t_{2g} holes, 4 $3d$ e_g^O holes, and no holes in $4p$ orbitals, near 1 t_{2g} hole and 1.5 e_g^O holes move to the Se atoms. The covalency is larger for states of e_g^O symmetry due to the larger hopping.

The first excited state is a spin triplet and orbital doublet of e_g symmetry, which lies 15.8 meV above the ground state. It is adiabatically connected with the Cr^{4+} state with one e_g electron and one electron in the $3d$ orbital of $3z^2-r^2$ symmetry. The charges of the three low-lying states for spin projection 1 are displayed in Table III. As shown in Table II, the average of the charges among the three states is in good agreement with the DFT calculations. The average compares better than the ground state values because the excitation energy is smaller than the broadening of the levels due to effective Cr-Cr hopping.

The ground state of the VSe_6 cluster is composed by a spin and orbital doublet, with spin $1/2$ and e_g symmetry respectively. The distribution of holes among the different $3d$ spin orbitals is in Table I for one of these four degenerate states. The corresponding distribution for the other states is obtained by symmetry, either interchanging simultaneously xz with yz and xy with x^2-y^2, or spin up and down, or both. As discussed before, the degree of spin polarization is larger for the cluster than for the DFT calculation, due to the limitations of the latter to represent an isolated V impurity. The ground state is connected adiabatically with the V^{4+} state with one electron of spin up or down in a linear combination of xz and xy orbitals, or the same combination replacing xz by yz and xy by x^2-y^2 (the two partners of an e_g doublet). In the real system, the magnetic interactions with neighboring Cr atoms, fixes the spin, but not the orbital which remains degenerate, since the Cr atoms are in an orbital singlet (of extended rather than localized nature).

The first excited state is a spin doublet and orbital a_{1g} singlet, which in the ionic limits corresponds to one electron occupying the $3z^2-r^2$ orbital. The excitation energy is 30.8 meV. This is more than one order of magnitude larger than the Kondo temperature T_K estimated from the fits of the resistivity discussed in Sec. II. Therefore, the expected Kondo effect is of SU(2) nature rather than SU(3), which corresponds to zero splitting (as for O_h symmetry in which the three t_{2g} orbitals are degenerate). A study of the SU(4) to SU(2) transition as a function of the splitting δ between two doublets, shows that the relevant parameter for the splitting is δ/T_K^0, where T_K^0 is the Kondo temperature for $\delta = 0$.[20,23]

IV. SUMMARY AND DISCUSSION

The observed resistance as a function of temperature of $CrSe_2$ with substitutional V impurities, and its dependence with magnetic field and temperature, is consistent with a purely orbital Kondo effect, in which the spin is quenched by the antiferromagnetic order, and the orbital degeneracy of the V impurity plays the role of a localized pseudospin, which is screened by conduction electrons. This situation is similar to the orbital Kondo effect detected by scanning tunneling microscopy studies of the ferromagnetic Cr(001) surface,[26,27] which is a consequence of the degeneracy between surface $3d$ states of xz and yz symmetry. It is also related to the observation of a Kondo resonance peak in photoemission studies of V-doped Cr,[28] although in this case the valence of Cr and V is quite different.

Due to the computational cost in obtaining the maximally localized Wannier functions, we could not use a unit cell large enough for the DFT calculations that would correspond to the dilute limit of substitutional V impurities. However, from these calculations complemented with many-body ones for a local VSe_6 cluster, we infer that two degenerate localized V states exist near the Fermi energy. The physical picture is the same as if the electron of V^{4+} could occupy one of two levels (either xy with some admixture of xz, or x^2-y^2 with a part of yz) with spin determined by the magnetic interactions. The screening of this orbital degree of freedom gives rise to the Kondo effect. The system is actually covalent, but the ionic picture reproduces the correct symmetry of the relevant

many-body states. This ionic picture permits a simple understanding of the fact that substitution of Ti does not lead to a Kondo effect, since Ti^{4+} has no d electrons and therefore, it is already a spin and orbital singlet, leaving no degree of freedom for screening of the conduction electrons.

A theoretical estimate of the Kondo temperature T_K is quite difficult. It depends exponentially on the effective exchange interaction J_K, which in turn depends on the precise energies for adding or removing an electron at the V site, and the mixture of these processes with the conduction electrons at the Fermi energy. Fit of the resistance curves gives values of T_K between 3 and 14 K.

For the electronic structure calculations, we have fixed the lattice parameters as those corresponding to pure $CrSe_2$,[10] and relaxed the ionic positions. Addition of a substantial amount of V or Ti substitutional impurities changes the lattice parameters,[10] but is not expected to change the local geometry around the impurities. Local distortions which change the symmetry would destroy the orbital degeneracy and with it the orbital Kondo effect, but this seems inconsistent with the experimental observations. For the case of an isolated molecule with partial occupation of degenerate levels, one expects the Jahn-Teller effect,[64] which consists in a spontaneous distortion that lowers the symmetry. In the solid, the elastic energy cost is larger and the energy gain is smaller due to the larger number of atoms involved in the collective distortion. If this energy gain is larger than that of the orbital Kondo effect (of the order of T_K), the latter would disappear. An estimation of the energy involved in the Jahn-Teller effect would require a calculation of the cost in elastic energy of the distortion and is beyond the scope of the present work.

A confirmation of the orbital Kondo effect could be obtained from spectroscopic measurements which can confirm the presence of a Kondo resonance at the Fermi energy. Unfortunately this requires good monocrystals and we could not succeed in their preparation. In any case, we expect that our results can stimulate further research on this issue.

ACKNOWLEDGMENTS

M.N. and A.A.A. are partially supported by CONICET, Argentina. D.C.F. gratefully acknowledges support from the Brazilian agencies CAPES and CNPQ. This work was sponsored by the project TetraFer ANR-09-BLAN-0211 of the Agence Nationale de la Recherche of France, PIP 112-200801-01821 of CONICET, and PICT 2010-1060 and PICT PRH 0102 of the ANPCyT-Argentina.

APPENDIX: CHANGE OF BASIS FOR O_h SYMMETRY

If the structure of $CrSe_2$ is compressed along the z axis, reducing the ratio of lattice parameters by 6.4%, the $CrSe_6$ octahedra formed by a Cr atom and its six nearest-neighbor Se atoms (see Fig. 9) becomes a perfect octahedron, with O_h symmetry. The energy of the 3d levels of Cr or substitutional V can be understood as a first approximation, as a perturbation of those of O_h symmetry when the octahedron is elongated along the z direction, reducing its symmetry to D_{3d}. As known, in O_h symmetry the five 3d levels split into a low-lying t_{2g} orbital triplet and an excited e_g^O doublet, where we use the superscript O to distinguish this irreducible representation from the e_g of D_{3d} . The natural choice of basis for the t_{2g} orbitals is $x'y'$, $x'z'$, and $y'z'$, where the primed coordinates point towards the Se atoms (see Fig. 9). The change of basis chosen in this figure is

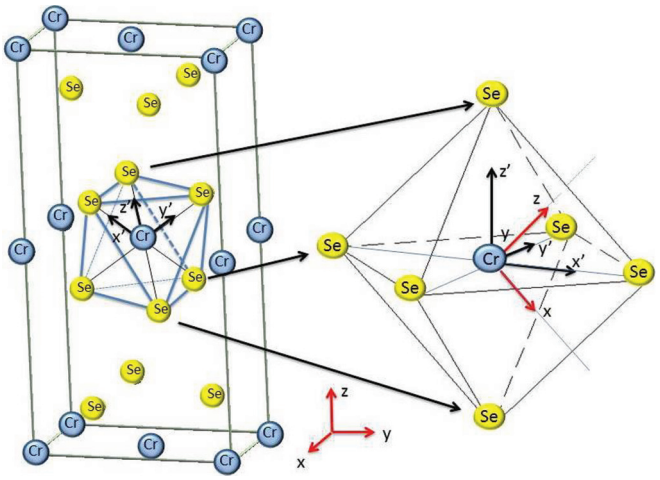

FIG. 9. (Color online) Illustration of the $CrSe_6$ octahedron, its position in the structure of $CrSe_6$, and the change of coordinate axis.

$$\begin{aligned} x' &= \frac{1}{\sqrt{2}}x - \frac{1}{\sqrt{6}}y + \frac{1}{\sqrt{3}}z, \\ y' &= \frac{\sqrt{2}}{\sqrt{3}}y + \frac{1}{\sqrt{3}}z, \\ z' &= -\frac{1}{\sqrt{2}}x - \frac{1}{\sqrt{6}}y + \frac{1}{\sqrt{3}}z. \end{aligned} \tag{A1}$$

With this change of coordinates, the 3d states in both bases become related by

$$\begin{aligned} \left|\frac{z'^2 - x'^2}{2}\right\rangle &= \frac{\sqrt{2}}{\sqrt{3}}|xz\rangle - \frac{1}{\sqrt{3}}|xy\rangle, \\ \left|\frac{3y'^2 - r'^2}{2\sqrt{3}}\right\rangle &= \frac{\sqrt{2}}{\sqrt{3}}|yz\rangle - \frac{1}{\sqrt{3}}\left|\frac{x'^2 - y'^2}{2}\right\rangle, \\ \left|\frac{x'y' - y'z'}{\sqrt{2}}\right\rangle &= \frac{1}{\sqrt{3}}|xz\rangle + \frac{\sqrt{2}}{\sqrt{3}}|xy\rangle, \\ \left|\frac{x'y' + y'z' - 2x'z'}{\sqrt{6}}\right\rangle &= \frac{1}{\sqrt{3}}|yz\rangle + \frac{\sqrt{2}}{\sqrt{3}}\left|\frac{x'^2 - y'^2}{2}\right\rangle, \\ \left|\frac{x'y' + x'z' + y'z'}{\sqrt{3}}\right\rangle &= \left|\frac{3z^2 - r^2}{2\sqrt{3}}\right\rangle. \end{aligned} \tag{A2}$$

The first members of the first two equations are the e_g^O states of O_h. Clearly the second members have the symmetry of xz and yz which transform like the double degenerate representation e_g of D_{3d}. The first members of the last three equations correspond to the t_{2g} states. From the second members one realizes that in D_{3d}, these states split into an e_g doublet (third and fourth equations) and an a_{1g} singlet (last equation).

*Present address: Centro Brasileiro de Pesquisas Físicas, Rua Dr. Xavier Sigaud, 150, Rio de Janeiro, RJ 22290-180, Brazil.
[1]J. G. Bednorz and K. A. Muller, Z. Phys. B **64**, 189 (1986).
[2]M. K. Wu, J. R. Ashburn, C. J. Torng, P. H. Hor, R. L. Meng, L. Gao, Z. J. Huang, Y. Q. Wang, and C. W. Chu, Phys. Rev. Lett. **58**, 908 (1987).
[3]Y. Kamihara, T. Watanabe, M. Hirano, and H. Hosono, J. Am. Chem. Soc. **130**, 3296 (2008).
[4]I. Terasaki, I. Tsukada, and Y. Iguchi, Phys. Rev. B **65**, 195106 (2002).
[5]M. Mikami, M. Yoshimura, Y. Mori, T. Sasaki, R. Funahashi, and M. Shikano, Jpn. J. Appl. Phys., Part 1 **42**, 7383 (2003).
[6]K. Takada, H. Sakurai, E. Takayama-Muromachi, F. Izumi, R. A. Dilanian, and T. Sasaki, Nature (London) **422**, 53 (2003).
[7]M. L. Kiesel, C. Platt, W. Hanke, and R. Thomale, Phys. Rev. Lett. **111**, 097001 (2013).
[8]A. Bourgeois, A. A. Aligia, and M. J. Rozenberg, Phys. Rev. Lett. **102**, 066402 (2009).
[9]K. Rościszewski and A. M. Oleś, J. Phys. Condens. Matter **25**, 345601 (2013).
[10]D. C. Freitas, M. Nuñez, P. Strobel, A. Sulpice, R. Weht, A. A. Aligia, and M. Nuñez-Regueiro, Phys. Rev. B **87**, 014420 (2013).
[11]A. C. Hewson, *The Kondo Problem to Heavy Fermions* (Cambridge University Press, Cambridge, 1993).
[12]J. Kondo, Progr. Theor. Phys. **32**, 37 (1964).
[13]D. C. Ralph and R. A. Buhrman, Phys. Rev. Lett. **69**, 2118 (1992).
[14]P. Jarillo-Herrero, J. Kong, H. S. J. van der Zant, C. Dekker, L. P. Kouwenhoven, and S. De Franceschi, Nature (London) **434**, 484 (2005).
[15]J. S. Lim, M.-S. Choi, M. Y. Choi, R. López, and R. Aguado, Phys. Rev. B **74**, 205119 (2006).
[16]F. B. Anders, D. E. Logan, M. R. Galpin, and G. Finkelstein, Phys. Rev. Lett. **100**, 086809 (2008).
[17]S. Lipinski and D. Krychowski, Phys. Rev. B **81**, 115327 (2010).
[18]C. A. Büsser, E. Vernek, P. Orellana, G. A. Lara, E. H. Kim, A. E. Feiguin, E. V. Anda, and G. B. Martins, Phys. Rev. B **83**, 125404 (2011).
[19]M. Karolak, D. Jacob, and A. I. Lichtenstein, Phys. Rev. Lett. **107**, 146604 (2011).
[20]L. Tosi, P. Roura-Bas, and A. A. Aligia, Physica B **407**, 3259 (2012).
[21]K. Grove-Rasmussen, S. Grap, J. Paaske, K. Flensberg, S. Andergassen, V. Meden, H. I. Jorgensen, K. Muraki, and T. Fujisawa, Phys. Rev. Lett. **108**, 176802 (2012).
[22]G. C. Tettamanzi, J. Verduijn, G. P. Lansbergen, M. Blaauboer, M. J. Calderón, R. Aguado, and S. Rogge, Phys. Rev. Lett. **108**, 046803 (2012).
[23]P. Roura-Bas, L. Tosi, A. A. Aligia, and P. S. Cornaglia, Phys. Rev. B **86**, 165106 (2012).
[24]E. Minamitani, N. Tsukahara, D. Matsunaka, Y. Kim, N. Takagi, and M. Kawai, Phys. Rev. Lett. **109**, 086602 (2012).
[25]A. M. Lobos, M. Romero, and A. A. Aligia, arXiv:1305.4169.
[26]O. Yu. Kolesnychenko, R. de Kort, M. I. Katsnelson, A. I. Lichtenstein, and H. van Kempen, Nature (London) **415**, 507 (2002).
[27]O. Yu. Kolesnychenko, G. M. M. Heijnen, A. K. Zhuravlev, R. de Kort, M. I. Katsnelson, A. I. Lichtenstein, and H. van Kempen, Phys. Rev. B **72**, 085456 (2005).
[28]G. Adhikary, R. Bindu, S. K. Pandey, and K. Maiti, Europhys. Lett. **99**, 37009 (2012).
[29]C. F. Van Bruggen, R. J. Haange, G. A. Wiegers, and D. K. G. De Boer, Physica **99B**, 166 (1980).
[30]T. Sekitani, M. Naito, and N. Miura, Phys. Rev. B **67**, 174503 (2003).
[31]S. Sanfilippo, H. Elsinger, M. Nuñez-Regueiro, O. Laborde, S. LeFloch, M. Affronte, G. L. Olcese, and A. Pelenzona, Phys. Rev. B **61**, R3800 (2000).
[32]P. Hohenberg and W. Kohn, Phys. Rev. **136**, B864 (1964).
[33]P. Giannozzi *et al.*, J. Phys.: Condens. Matter **39**, 395502 (2009).
[34]D. Vanderbilt, Phys. Rev. B **41**, 7892 (1990).
[35]J. P. Perdew, K. Burke, and M. Ernzerhof, Phys. Rev. Lett. **77**, 3865 (1996).
[36]J. P. Perdew and A. Zunger, Phys. Rev. B **23**, 5048 (1981).
[37]D. M. Ceperley and B. J. Alder, Phys. Rev. Lett. **45**, 566 (1980).
[38]C. M. Fang, C. F. Van Bruggen, R. A. de Groot, G. A. Wiegers, and C. Haas, J. Phys.: Condens. Matter **9**, 10173 (1997).
[39]S. Nakatsuji, Y. Nambu, H. Tonomura, O. Sakai, S. Jonas, C. Broholm, H. Tsunetsugu, Y. Qiu, and Y. Maeno, Science **309**, 1697 (2005).
[40]H. J. Monkhorst and J. D. Pack, Phys. Rev. B **13**, 5188 (1976).
[41]N. Marzari and D. Vanderbilt, Phys. Rev. B **56**, 12847 (1997).
[42]A. Ferretti *et al.*, computer code WANT, http://www.wannier-transport.org.
[43]A. Calzolari, N. Marzari, I. Souza, and M. Buongiorno Nardelli, Phys. Rev. B **69**, 035108 (2004).
[44]V. I. Anisimov, J. Zaanen, and O. K. Andersen, Phys. Rev. B **44**, 943 (1991); V. I. Anisimov, I. V. Solovyev, M. A. Korotin, M. T. Czyzyk, and G. A. Sawatzky, *ibid.* **48**, 16929 (1993); A. I. Liechtenstein, V. I. Anisimov, and J. Zaanen, *ibid.* **52**, R5467 (1995).
[45]M. Cococcioni and S. de Gironcoli, Phys. Rev. B **71**, 035105 (2005).
[46]A. G. Petukhov, I. I. Mazin, L. Chioncel, and A. I. Lichtenstein, Phys. Rev. B **67**, 153106 (2003).
[47]A. A. Aligia and T. Kroll, Phys. Rev. B **81**, 195113 (2010).
[48]A. A. Aligia, Phys. Rev. B **88**, 075128 (2013).
[49]J. H. Jefferson, H. Eskes, and L. F. Feiner, Phys. Rev. B **45**, 7959 (1992).
[50]M. E. Simon and A. A. Aligia, Phys. Rev. B **48**, 7471 (1993).
[51]V. I. Belinicher, A. L. Chernyshev, and L. V. Popovich, Phys. Rev. B **50**, 13768 (1994).
[52]L. F. Feiner, J. H. Jefferson, and R. Raimondi, Phys. Rev. B **53**, 8751 (1996), and references therein.
[53]M. E. Simon, A. A. Aligia, and E. R. Gagliano, Phys. Rev. B **56**, 5637 (1997), and references therein.
[54]A. A. Aligia, M. E. Simon, and C. D. Batista, Phys. Rev. B **49**, 13061 (1994).
[55]K. I. Kugel and D. I. Khomskii, Sov. Phys. Usp. **25**, 231 (1982).
[56]A. A. Aligia and M. A. Gusmão, Phys. Rev. B **70**, 054403 (2004).

[57] S. Landron and M. B. Lepetit, Phys. Rev. B **74**, 184507 (2006); **77**, 125106 (2008).
[58] O. Eriksson, M. S. S. Brooks, and B. Johansson, Phys. Rev. B **41**, R7311 (1990).
[59] H. Eschrig, M. Sargolzaei, K. Koepernik, and M. Richter, Europhys. Lett. **72**, 611 (2005), and references therein.
[60] G. Nicolas, J. Dorantes-Dávila, and G. M. Pastor, Phys. Rev. B **74**, 014415 (2006).
[61] S. Sugano, Y. Tanabe, and H. Kamimura, *Multiplets of Transition Metal Ions in Cristals* (Academic Press, New York, 1970), Chap. X.
[62] J. C. Slater and G. F. Koster, Phys. Rev. **94**, 1498 (1954); R. R. Sharma, Phys. Rev. B **19**, 2813 (1979).
[63] J. M. Eroles, C. D. Batista, and A. A. Aligia, Phys. Rev. B **59**, 14092 (1999).
[64] H. Jahn and E. Teller, Proc. R. Soc. London, Ser. A **161**, 220 (1937).